RSC Advances

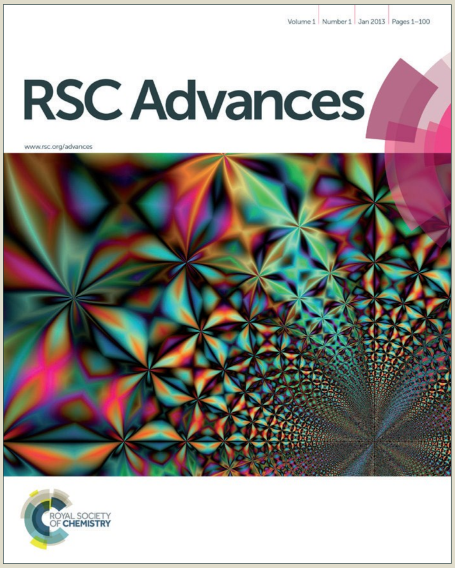

ROYAL SOCIETY OF CHEMISTRY

www.rsc.org/advances

Synthesis of a unique cross-linked polyzwitterion/anion having aspartic acid residue and its use for Pb^{2+} removal from aqueous solution

Zakariyah A. Jamiu, Tawfik A. Saleh*, Shaikh A. Ali *

Department of Chemistry, King Fahd University of Petroleum & Minerals, Dhahran, Saudi Arabia

**Corresponding authors*

E-mail address: tawfik@kfupm.edu.sa

Fax: (966) 13 860 1734
Home Page: http://faculty.kfupm.edu.sa/CHEM/tawfik/

E-mail address: shaikh@kfupm.edu.sa

Fax: (966) 13 860 2436
Home Page: http://faculty.kfupm.edu.sa/CHEM/shaikh/

Abstract

In this work, a unique cross-linked polyzwitterion/anion having aspartic acid residue was synthesized via butler's cyclopolymerization protocol involving *N,N*-diallylaspartic acid hydrochloride, 1,1,4,4-tetraallylpiperazinium dichloride and sulfur dioxide in the presence of azoisobutyronitrile. The structure and morphology of the polymer were characterized by using FTIR, TGA, EDX and SEM. The adsorption performance of the resin was evaluated using lead Pb(II) as model. The effect of various parameters such as contact time, pH, initial concentration and temperature were investigated to arrive at optimum conditions. Optimum pH of 6.0 and dosage of 1.5g L^{-1} were obtained. The mechanism of adsorption was investigated using kinetic, diffusion, isotherm and thermodynamic models. The adsorption kinetic data were described well by the pseudo-second order model with R^2 of 0.999. The activation energy (Ea) of the adsorption process was calculated as 39.29 kJ mol^{-1}. The negative ΔG^o values indicate a spontaneous adsorption process while the negative ΔH^o (-43.87 KJ/mol) suggests an exothermic reaction. Adsorption data were described well by the Langmuir and Temkin models. EDX analysis confirmed the adsorption of Pb^{2+}on the polymer. The overall results suggest that the polymer could be employed as an efficient adsorbent for the adsorption of toxic Pb^{2+} from polluted aqueous solutions.

Keywords: cross-linked polyzwitterion/anion, resin, sorption, kinetics, isotherm, thermodynamic

1. Introduction

Heavy metals are released into the surface and ground water because of various activities such as electroplating, and pigment and paint manufacturing. Because of their toxicity and tendency to bioaccumulation, the removal of metals from industrial effluents before discharge into the environment is required to mitigate any impact on plants, animals and humans [1]. Lead is one of the most toxic metals that are widely used in various industries, such as battery and glass manufacturing, metal plating and finishing, printing and tanning. The permissible levels of lead in drinking and waste water are 0.005 mg/L and 0.05mg/L, respectively [2].

Several conventional methods, such as chemical precipitation as hydroxides, carbonates or sulfides and subsequent liquid-solid separation, sorption, membrane processes, and reverse osmosis, electrolytic recovery and liquid-liquid extraction, are used for the removal of pollutants [3]. However, these technologies are either expensive for the treatment and disposal of the secondary toxic sludge or ineffective when the toxic metal is present in wastewaters at low concentrations [4].

Alternatively, adsorption is one of the preferred methods for the treatment of wastewater because of its efficiency and simplicity. A successful adsorption process depends on the adsorption performance of the adsorbents. Various conventional adsorbents have been reported for the removal of lead from wastewaters including activated carbon, clay, metal oxides nanoparticles and nanomaterials [3, 5-7]. However, small particle size of nanoparticle results in the difficulty of separation from solution, which limits the application in water treatment. The new adsorbents requested by the industry should have high capacity, rapid adsorption kinetics and operational stability at elevated temperatures in the presence of steam and other reaction components. The new adsorption processes may then take advantage of such materials.

Among these, polymers could represent the best candidate displaying a pronounced chemical versatility given by the great number of chemical functionalities or motifs present in their structures. Recently, researchers have focused on the syntheses of zwitterionic cross-linked inorganic and/or organic hybrid polymer materials for the removal of heavy metal ions via electrostatic effects [8-10]. Considerable attention has been given to synthesize chelating agents containing amino methyl phosphonate motif owing to its extraordinary chelating properties in extracting heavy metal ions from wastewater. More recently, a porous resin with Schiff base chelating groups for removal of heavy metal ions from aqueous solutions has been synthesized [11].

The objective of the current work was to synthesize a novel functionalized resin as sorbent for removal of Pb^{2+} ions as a model case from aqueous solution. The cross-linked polymer is anticipated to retain the metal chelating character of the nitrogen in addition to the two anionic centers in the carboxylates in aspartic acid. In this respect, we intend to apply Butler's homo-[12-15] and co-cyclopolymerization [16-18] protocol, which is instrumental in converting diallylammonium salts into a plethora of industrially significant cyclopolymers, whose pyrrolidine ring-embedded architecture is considered to be the eighth most important structural type [19, 20]. Butler's cyclopolymer poly(diallyldimethylammonium chloride) has numerous publications and patents (> 1000). Water purification and personal care formulation remain the important areas of its application [12]. With this in mind, herein we report the cycloterpolymerization of diallyl monomer 1, cross-linker **2** and SO_2 to generate a novel pH-responsive cross-linked cycloterpolymer **4** (Scheme 1). The cyclopolymerization protocol was used for the first time to obtain resin **4** containing the residues of aspartic acid with all its basic centers intact.

2. Experimental

2.1 Chemicals and Materials

Azoisobutyronitrile (AIBN) from Fluka AG was purified by crystallization from a chloroform–ethanol mixture. Dimethylsulfoxide (DMSO) was dried over calcium hydride overnight and then distilled under reduced pressure at a boiling point of 64–65°C (4 mm Hg). Standard solution (1000 mg/L) of Pb (II), hydrochloric acid, nitric acid and sodium hydroxide were obtained from

Sigma–Aldrich. The lead standard solution was utilized to prepare the required initial concentrations by dilution. All solvents used were of analytical grade.

2.2 Physical methods

Field emission scanning electron microscope (FESEM) was used to characterize the surface morphology of the polymer before and after the adsorption of lead. Energy-dispersive X-ray spectroscope (EDX) equipped with a detector model X-Max was employed to obtain the elemental spectrum and to get elemental analysis of the pristine polymer and Pb(II)-loaded polymer. PerkinElmer 2400 Series II CHNS/O Elemental Analyzer was also used for the elemental analysis. Thermo Scientific iCE 3000 flame atomic absorption spectrometer (FAAS) equipped with a 10 cm air-acetylene burner was used to monitor the concentration of Pb(II). The concentrations of some metal ions in real wastewater samples was analysed by inductively coupled plasma mass spectrometry (ICP-MS) model ICP-MS XSERIES-II Thermo Scientific. IR spectra were recorded on a Perkin–Elmer 16F PC FTIR spectrometer. 1H and 13C spectra were measured on a JEOL LA 500 MHz spectrometer using HOD signal at d4.65 and dioxane signal at 67.4 ppm as internal standards, respectively. Thermogravimetric analysis (TGA) was carried out using a thermal analyzer SDT Q600, V20.9 Build 20 manufactured by TA instruments, USA. The temperature was raised at a uniform rate of 10°C/min. The analyses were made over a temperature range of 20–700°C in an air-atmosphere flowing at a rate of 100 mL/min. The specific surface area and pore size distribution were determined by the Brunauer-Emmett-Teller (BET) and Barrett-Joyner-Halenda (BJH) methods, respectively.

2.3 Synthesis

To the best of our knowledge, the following synthesis of the resins would represent the first example of cross-linked cyclopolymer containing the residues of aspartic acid by the cyclopolymerization protocol involving monomers having unquenched nitrogen valency. The cross-linker **2** was prepared as described [21]. Monomer **1** containing the residue of aspartic acid was prepared *via* Michael addition of diallylamine to dimethyl maleate followed by hydrolysis of the Michael adduct in aqueous NaOH and neutralization with aqueous HCl.

2.3.1. General procedure for the terpolymerization of 1 and 2 with sulfur dioxide.

To a solution of monomer **1** (6.06 g, 24.2 mmol), cross-linker **2** [21] (0.582 g, 1.82 mmol) in DMSO (9.1 g) in a round bottom flask (50 ml), was absorbed SO_2 (1.78 g, 27.8 mmol) (from a cylinder) by gentle blowing it over the stirred surface of the solution (scheme 1). After the initiator AIBN (105 mg) was added, the reaction mixture was stirred at 60^oC under N_2 for 24 h. Within 3-5 h, the magnetic stir-bar stopped moving; the reaction mixture became a transparent swelled gel. At the end of the elapsed time, the swelled gel of the cross-linked polyzwitterionic acid (CPZA) **3** was soaked in water (48 h) with replacement of water several times. The swelled gel in water (≈65 cm^3) was agitated with NaOH (1.6 g, 40 mmol) at room temperature for 5 h followed by further addition of NaOH (1.6 g, 40 mmol) and stirring for 1 h to ensure complete exchange with Na^+. The CPZA **3** in acid form is less expanded owing to the zwitterionic form while the anionic form in resin CDAP **4** is highly expanded in the above alkaline mixture. The resin **4** was dropped onto acetone (200 ml), filtered, dried at 60°C under vacuum to a constant weight (7.7 g, 90%). (Elemental analysis Found: C, 38.1; H, 4.6; N, 4.4; S, 9.5%). A terpolymer from momomer **1** in disodium form $C_{10}H_{13}NNa_2O_4$ (93 mol%) and monomer **2** in the hydroxide form $C_{16}H_{30}N_2O_2$ (7 mol%) and SO_2 (100 mol%) requires C, 38.65; H, 4.41; N, 4.62; S, 9.93).

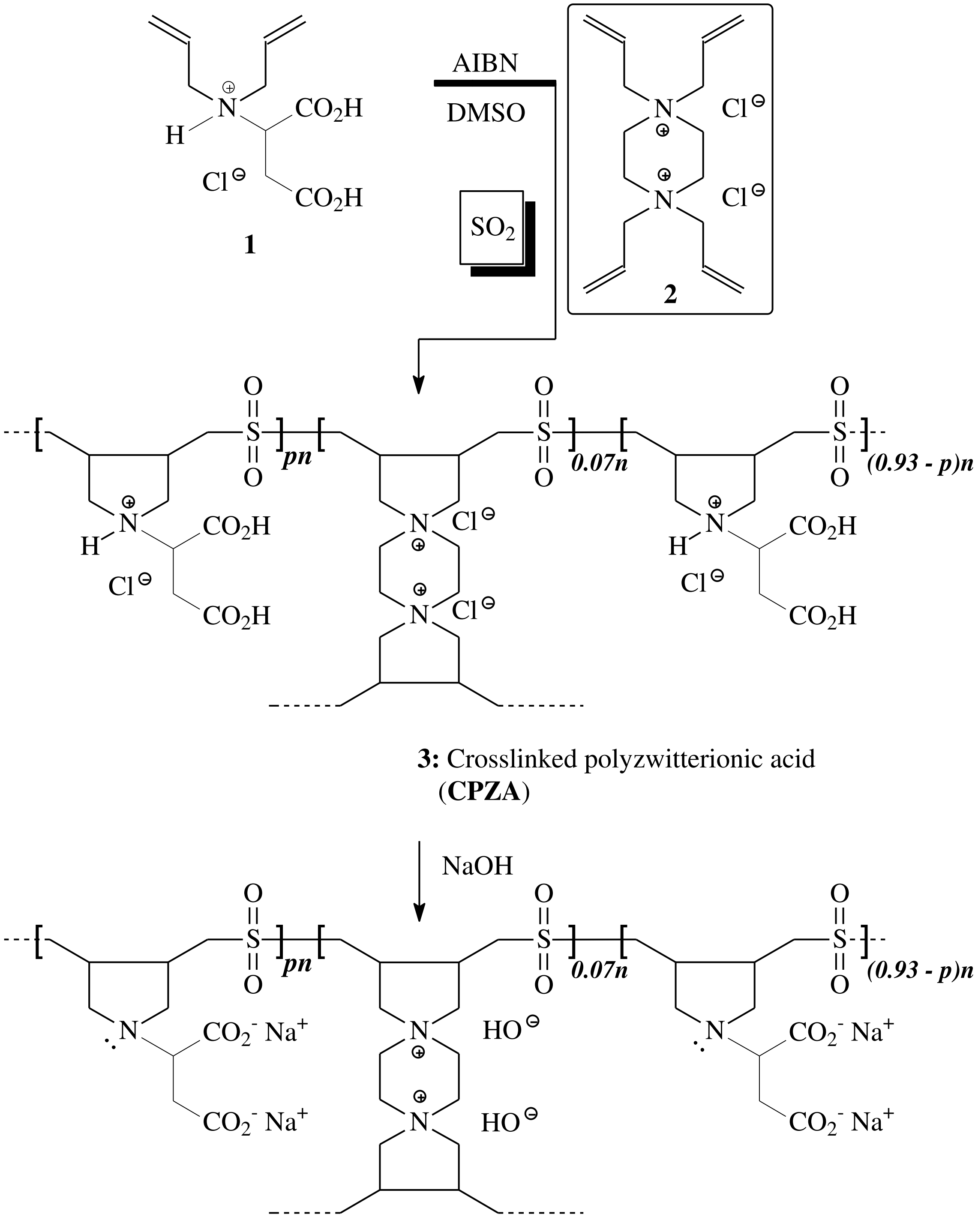

3: Crosslinked polyzwitterionic acid (**CPZA**)

4: Crosslinked dianionic polyelectrolyte (**CDAP**)

Scheme 1. Synthesis of cross-linked polyzwitterion/anion polymers.

2.4 Adsorption of Pb(II) on CDAP

The experiments were carried out as follow. A 30mg of adsorbent CDAP was added in 20mL of aqueous Pb^{2+} solution of specific concentration and then stirred for period of 2, 5, 10,15, 20, 30, 40, 50, 60, 90 and 120 min respectively at 298 K. This study was carried out with different initial Pb^{2+}concentrations ranging from 10 to 100 mgL^{-1} while maintaining the adsorbent amount of 1.5 g L^{-1}. The resultant solution was filtered using a filter paper and the filtrate was analyzed by atomic absorption spectroscopy to determine the amount of Pb^{2+} uptake. The pH of the solution was also measured during course of adsorption. The effect of pH was studied at 298K with an initial Pb^{2+} concentration of 40 mgL^{-1}. The kinetic and thermodynamic behaviors were studied in a similar manner with initial Pb^{2+} concentration of 40 mgL^{-1} at 298, 313 and 333K respectively. The amount of Pb^{2+} adsorbed by the adsorbent CDAP was computed using the following equation.

$$q_t = \frac{(C_i - C_t)V}{W} \qquad (1)$$

Here, C_i and C_t are the initial and final concentrations of Pb^{2+} ions in mg L^{-1} respectively; V is the volume of solution in L with which the resin of weight W in gram is contacted and q_t is the adsorption capacity in mg g^{-1}.

2.5 Regeneration of the Resin

Adsorption experiments were performed by stirring 0.5 g of the resin in aqueous 333 ml Pb^{2+} solution for 120 min. The amount of Pb^{2+} uptake was determined as described above. The loaded resin was then filtered and dried at 60 °C under vacuum to a constant weight. It was then quantitatively transferred to a stirring 0.5 M HNO_3 (333 ml) for 120 min for the desorption experiment, this process was repeated two times. The regenerated resin was washed and dried and the amount of desorbed Pb^{2+} was determined. The efficiency of desorption process was calculated by taking the ratio of the desorbed amount to that of the adsorbed amount of Pb^{2+}. The re-usability of the regenerated resin was tested in a similar way to the adsorption experiment. All experiments were done in triplicates.

2.6 FTIR spectroscopy

The FT-IR spectra of the resin before and after adsorption experiments were examined. Unloaded resin (30 mg) was contacted with 40 mgL^{-1} Pb^{2+} concentration at adsorbent amount of 1.5 g L^{-1} for 120 min at a pH of 6.0. It was filtered and dried under vacuum until constant weight was achieved.

3.0 Results and discussion

3.1. Synthesis of cross-linked Terpolymer

Monomer **1**, cross-linker **2** and SO_2 underwent cycloterpolymerization to give cross-linked polyzwitterionic acid **3** (CPZA) which upon basification with NaOH afforded the cross-linked dianionic polyelectrolyte (CDAP) **4** in an excellent overall yield of 90% (Scheme 1). Resin **4** has the unquenched nitrogen valency, which can act as a chelation center along with the two carboxylate motifs. The synthesis represents the first example of a cross-linked cyclopolymer containing the residues of the versatile aspartic acid. The three basic centers (N and CO_2^-) in aspartic acid with different basicity constant is anticipated to impart interesting chelation properties in sequestrating toxic metal ions.

3.2. FT-IR Characterization of Monomers and Polymer

The IR spectrum of cross-linked polyzwitterionic acid **3** (CPZA) shows strong bands at 1727 cm^{-1} and 1631cm^{-1} which are usually attributed to the asymmetric and symmetric stretchings of COOH [22] fig. 1a. These bands were also observed for monomer 1 (spectrum not shown here). The resin **3** (CPZA) also contains bands at 1304 cm^{-1} and 1125 cm^{-1} which have been assigned in literature to asymmetric and symmetric bands of SO_2 [23]. In the unloaded cross-linked dianionic polyelectrolyte 4 CDAP, the C=O stretch shift dramatically to 1578.7 cm^{-1} and 1406.8 cm^{-1} for asymmetric and symmetric vibrations respectively because it is now in COO^- form (fig. 1b). After Pb^{2+} adsorption fig. 1c, an appreciable increase in the intensity and broadness of the COO^- bands is noted [24]. At CPZA, the band at 854.9 cm^{-1} is assigned to C-H bond vibration in the ring while the band at 639 cm^{-1} is assigned to N-H out of plane vibration [25]. The band at 878 cm^{-1} at CDAP, and the band at 875 cm^{-1} at Pb adsorbed CDAP, are assigned to C-H bond vibration in the ring. The slight shift could be attributed to the interaction between the nitrogen pair of electrons with lead metal ion leading to distortion of electron cloud in the neighboring C-H bond.

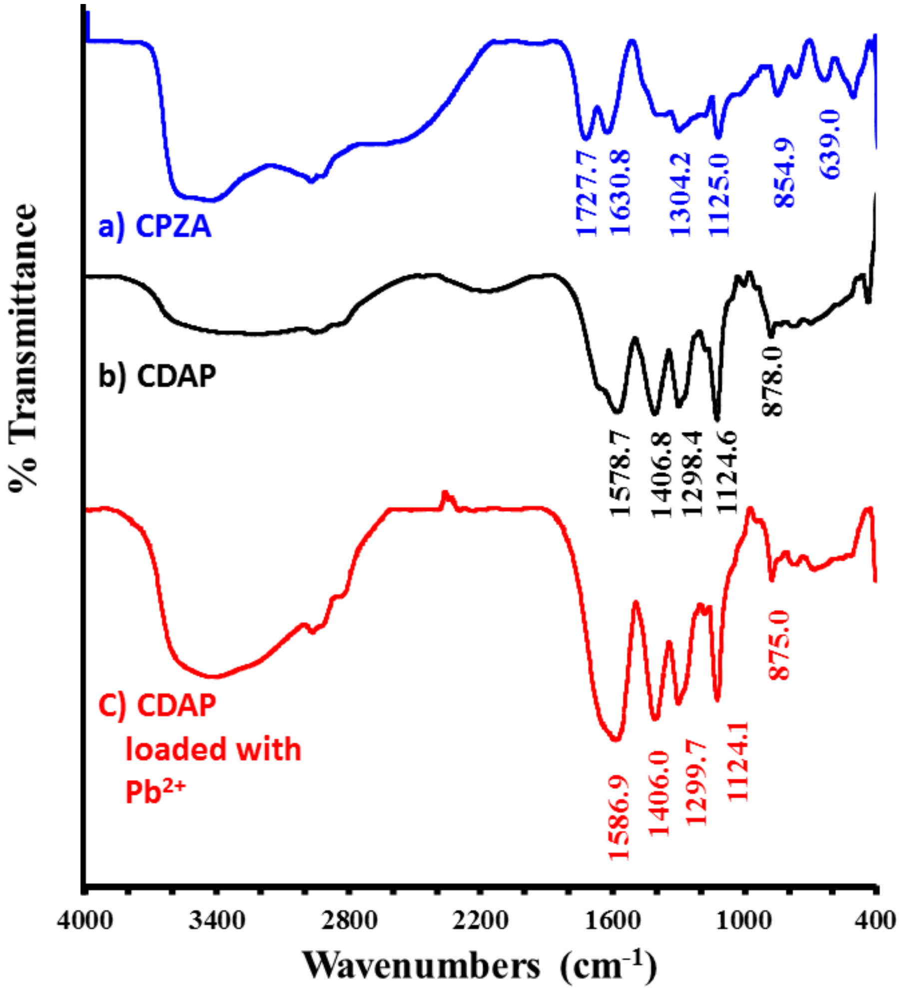

Figure 1. IR Spectra of cross-linked resins (a) CPZA 3 (b) CDAP 4 and (c) CDAP 4 loaded with Pb^{2+}

3.3. Thermogravimetric analysis (TGA)

Figure 2 shows the thermogravimetric analysis (TGA) curve of 4 (CDAP) with three distinct weight loss steps. The first slow but gradual weight loss of about 20% is attributed to the removal of moisture and water molecules embedded inside the cross-linked polymer. The second dramatic loss of about 25% around 320°C is attributed to the loss of SO_2 due to polymer degradation. The third slow and gradual loss of 15% is attributed to the combustion of nitrogenous organics with the release of NOx, CO_2 and H_2O gases [23]. At 700°C, the residual mass was found to be 40%.

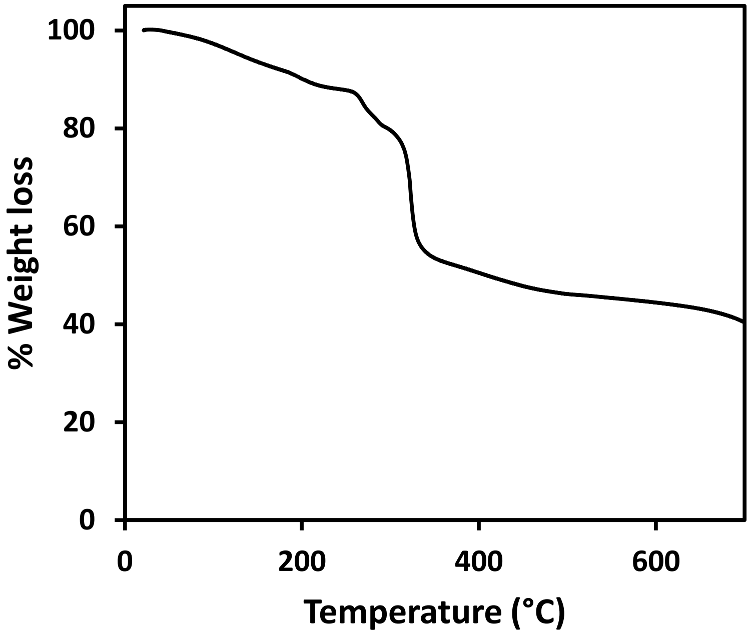

Figure 2: TGA curve of CDAP 4

3.4. Effect of pH on the adsorption

The relationship between the initial pH of solution and the percentage removal of Pb^{2+} is depicted in Figure 3. In the pH range of 3 - 9, the Pb^{2+} uptake was monitored by contacting the resin with $40mgL^{-1}$ lead (Pb^{2+}) solution for 15 min at room temperature. The percentage Pb^{2+} removal initially increased from 91.5% to 95.8% as the pH increased from 3 to 6. Further increase of pH to 9 saw a gradual decrease of Pb^{2+} uptake as percentage Pb^{2+} dropped to 94.9%. Therefore, the optimum pH is 6. It has been established that solution pH plays a critical role in metal ion adsorption process due to its influence on both the nature of the metal ions in solution and the state of the functional groups on the surface of the adsorbents [25]. Studies have identified three forms of lead species: Pb^{2+}, $Pb(OH)^+$ and $Pb(OH)_2$ in the pH range 2.0-8.0. The distribution of these species as calculated by MINEQL software shows that Pb^{2+} is the preponderant species at pH between 1 and 6 and that its hydrolysis to $Pb(OH)^+$ and $Pb(OH)_2$ starts as pH increases while $Pb(OH)_2$ dominates at the pH higher than 6.0 [26, 27]. Under low pH: (1) competition ensued between H^+ and Pb^{2+} and (2) the functional groups on the surface of the resin are in protonated forms which do not favor coordination with Pb^{2+} species as they are repelled by the electrostatic force. Thus, the Pb^{2+} absorption capacity of the resin is decreased [27]. As the pH is increased, this competition reduces and the functional groups on the resin are becoming less protonated, thereby making them more available for coordination with Pb^{2+}. This accounts for increased percentage removal that peaked pH 6.0. Beyond pH 6.0, there is deprotonation as basicity increases, and the functional groups are in anionic forms that should encourage greater coordination with Pb^{2+}. However, this didn't increase the percent Pb^{2+}removal as lead are now being hydrolysed into $Pb(OH)^+$ and $Pb(OH)^2$ thereby reducing the amount of free Pb^{2+} available for complexation. The rest of the adsorption experiments were carried out at the optimum pH of 6.0.

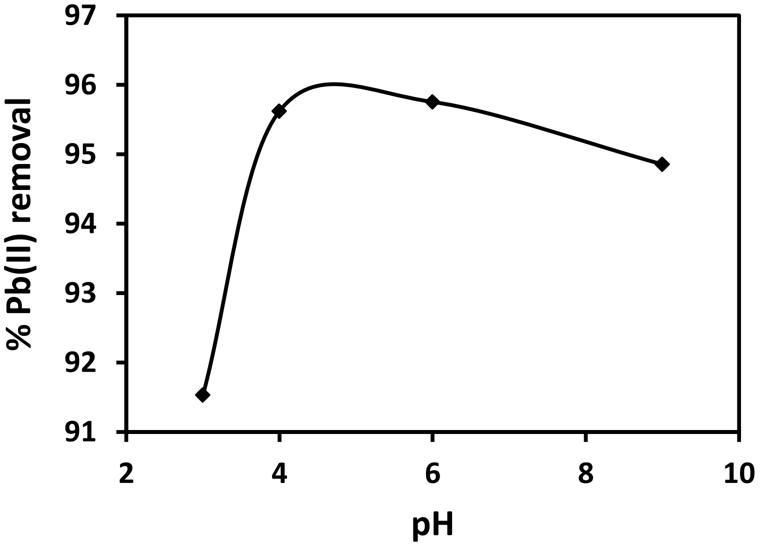

Fig. 3. Effect of pH on the adsorption of Pb^{2+} ions

3.5. Effect of initial concentration on the adsorption of Pb(II)

Figure 4(a) depicts the effect of initial concentration of Pb^{2+} on the percentage Pb^{2+} removal by CDAP 4. It can be seen that the percentage removal for the Pb2+ rapidly increases from 0 to about 25 min contact time and thereafter slowly until it reaches equilibrium. This is due to the fact that the adsorption kinetic depends on the surface area of the adsorbent which is largely uncovered at the start of the experiment (0 contact time). Therefore, the rate of adsorption at the early time increases rapidly until it reaches a point where the remaining fewer adsorption sites are competed for by lead ions. Hence the rate of adsorption slows down until it reaches equilibrium [28]. This situation is observed for all the initial concentration of lead ranging from 10-100 ppm. The effect of the amount of adsorbate was also investigated and it was observed that the adsorption capacity of CDAP 4 increases as the concentration of Pb^{2+} is raised from 10 up till 100 ppm (Figure 4b).

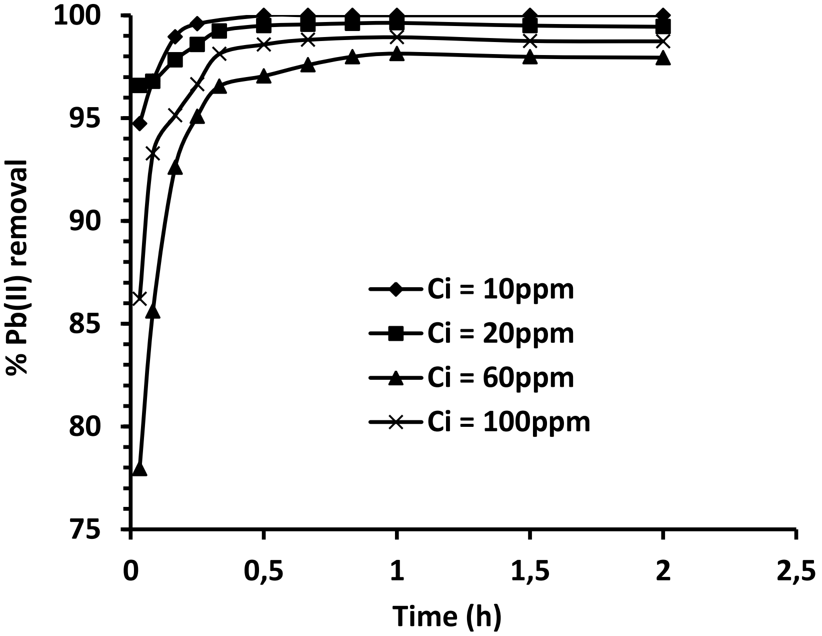

(a)

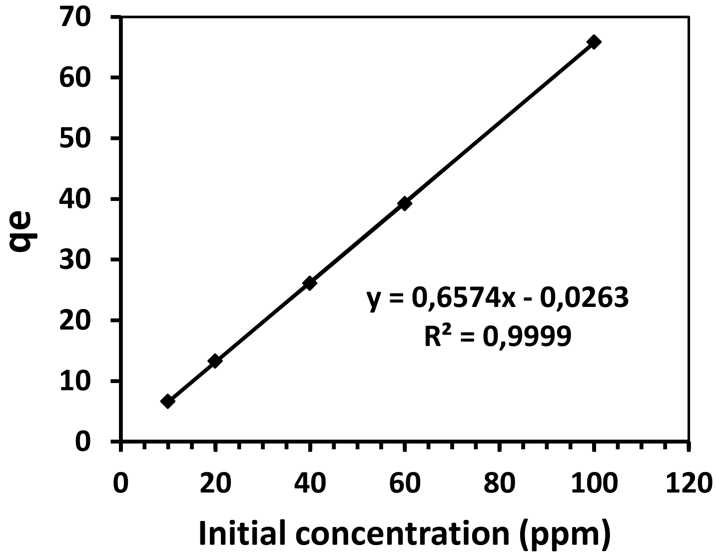

(b)

Fig. 4. (a) Effect of initial Pb^{2+} concentrations on percent Pb^{2+} removal (b) Effect of initial concentrations of Pb^{2+} on the adsorption capacity.

3.6. Adsorption kinetics

The dynamics of the interaction at the solid-solution interface during the adsorption of Pb^{2+} from aqueous solution can be described in terms of models. These kinetic models study the rate-controlling mechanism of the adsorption process that comprises of chemical reaction, mass transfer and diffusion control systems. Two kinetic models namely Pseudo first-order and Pseudo second-order have been used in this work to analyze the adsorption data of Pb^{2+} adsorption on CDAP.

3.6.1. Pseudo first-order (Lagergren) kinetics

Pseudo first-order relates the adsorption rate of solute to adsorption capacity of the adsorbent. The linear form of the equation is given by the following equation [29].

$$\log(q_e - q_t) = \log q_e - (\frac{k_1 t}{2.303}) \qquad (2)$$

Where q_e and q_t are the amounts of Pb^{2+} adsorbed in (mg g^{-1}) at equilibrium time and at any time, t, respectively and k_1 is the first order rate constant in (h^{-1}). A linear plot of log (qe – qt) versus t yields a straight line for the pseudo first-order kinetics from which k_1 and $q_{e,cal}$ are calculated. Figure 6(a) shows the combined Lagergren plots for the various initial concentrations of Pb^{2+} used for the kinetic studies when adsorbent amount is kept at 1.5gL^{-1}. The kinetic parameters extracted from these plots are displayed in Table 1. Judging from the fittings, it can be seen that there is generally good linearity of Lagergren Pseudo first-order plots as R^2 ranges from 0.95 to 0.99 for all the plots (Table 1). The rate constants k_1 are determined to vary between 2.7 to 16.38 h^{-1}. There is a general downward trend of k_1 as initial concentrations increase. However, considering the equilibrium adsorption capacities reveal a sharp disagreement between the experimentally observed $q_{e,exp}$ and that derived from Largergren pseudo first-order plots, $q_{e,cal\ 1}$, as shown in Table 1. This is understood to mean that even though, the model fits Pb^{2+} adsorption data quite fairly, it is not suitable for estimation of $q_{e,cal\ 1}$ as it is not a true first order equation where the intercept of the plot of log (q_e – q_t) versus t should be equal to log q_e as in equation 3 [30].

3.6.2. Pseudo second-order kinetics

The failure of Lagergren first-order kinetic model to correctly estimate the equilibrium adsorption capacity q_e drives us to pseudo second-order kinetic model for analysis of the dynamics. The linear form of the pseudo second order model [31] can be written as:

$$\frac{t}{q_t} = \frac{1}{k_2 q_e^2} + \frac{t}{q_e} \qquad (3)$$

Here, k_2 (g mg^{-1} h^{-1}) is pseudo second order rate constant, q_e and q_t are the adsorption capacities at equilibrium and at any time t respectively. A plot of t/q_t against t, Figure 6(b), gave linear relationship allowing for the calculation of q_e and k_2 as displayed in Table 1. The initial adsorption rate is also presented as $h = k_2 q_e^2$. As can be seen from Figure 6 (b) and Table 1, pseudo second-order model gave an excellent fitting for the adsorption data with the square of regression coefficient of unity for all the experiments. Interestingly, the calculated equilibrium adsorption capacities, $q_{e,cal\ 2}$, show very nice agreement with the experimentally observed, $q_{e,exp}$ Table 1. While this is an evidence that pseudo second order model describes very well the adsorption process taking place between CDAP 4 and Pb^{2+} ions, it also means that such adsorption process might be of chemical nature [32].

3.6.3. Intra-particle diffusion.

The Weber-Morris intraparticle diffusion was used as a model to evaluate the diffusion contribution of Pb^{2+} adsorption within the resin. A plot of q_t against $t^{1/2}$ (equation 5) should give a straight line if the mechanism of the adsorption is controlled by the diffusion of the adsorbate ions within the particle in the pore of the adsorbent [33, 34]. The diffusion process may take place in the external, macropore and micropore surfaces leading to multi-linear plots [35] suggesting that other processes might play roles in the adsorption [36].

$$q_t = k_{id} t^{1/2} + x_i \qquad (4)$$

where q_t is the adsorption capacity at any time t, k_{id} is the intraparticle diffusion rate constant (mg/g hr.) and x_i is a constant that takes into account the boundary layer thickness.

It can be seen from Figure 6(c) that the diffusion model exhibits three distinct parts for the duration of the study at different temperatures. The effects of temperature on the Weber-Morris parameters are displayed in Table 2. At 298K, from the start of the process, the first and second straight portions of the curve with steep slopes reflect the easy diffusion of Pb^{2+} ion inside the macropores of the CDAP resin while the third part, indicates the slow diffusion within the micropore [35]. It is informative to note that the third part shows a gradual approach to equilibrium which is an indication of a concentration dependent diffusion process [37]. This result is in agreement with pseudo-second order kinetic model. Experiments conducted at 313 and 333K show similar behavior but with gradual decrease in k_{id} and their regression coefficients (see Figure 6 (c) and Table 2). Obviously, this is an indication of the exothermic behavior of the adsorption process which slows down the diffusion mechanism as temperature rises.

3.7. Adsorption isotherm models

Isotherm models are used to explain the nature of adsorption sites, their interaction and the number of layer that may be formed on them. Among many models in literature, Lamgmuir, Freundlich and Tempkin isotherms were used for this study.

3.7.1. Langmuir Isotherm

The basic assumptions in Langmuir isotherm are that the adsorption is a monolayer type on a homogenous surface where the adsorption at one site is completely independent of the other [38]. It can be expressed in linear form as follows:

$$\frac{C_e}{q_e} = \frac{C_e}{Q_m} + \frac{1}{Q_m b} \qquad (5)$$

Where Q_m is the quantity of adsorbate required to form a single monolayer on a unit mass of the adsorbent (mg g^{-1}), Q_e is the amount adsorbed on a unit mass of adsorbent (mg g^{-1}) at equilibrium concentration C_e (mgL^{-1}) and b is an equilibrium constant that takes care of the apparent energy of adsorption. A plot of C_e/q_e against C_e yielded a straight line in agreement with Langmuir isotherm giving the isotherm parameters as depicted in Table 3. The high R^2 of about 0.99 is an indication of the suitability of this isotherm in explaining the equilibrium adsorption of Pb^{2+} onto the resin. It thus clarifies that it is a monolayer adsorption. Additional analysis was also made by using the dimensionless equilibrium parameter R_L that is a measure of the favorability of adsorption. R_L values are found to range from 0.09 to 0.90, which means that it is favorable adsorption process.

Comparison of adsorption capacities from the Langmuir isotherm of the current adsorbent for the removal of Pb(II) with those of other adsorbents reported in the literature is displayed in Table 5. Although it showed lower performance than some reported adsorbents of different nature [54-56], the polymer quite interestingly compares favorably with those adsorbents of similar nature and its reusability and environmental friendliness stand it out.

3.7.2. Freundlich Isotherm

Freundlich isotherm describes multilayer adsorption taking place on a heterogeneous surface. As in many systems, the heat of adsorption decreases with increasing extent of adsorption but this model unifies the energy [39]. The linear form is given as follows:

$$\log q_e = \log k_f + \frac{1}{n} \log C_e \qquad (6)$$

k_f is the Freundlich constant and n is the heterogeneity factor which is a measure of deviation from linearity. Table 3 shows a high n of about 2 which is far from unity and R^2 of 0.93. These collectively prove that Freundlich isotherm does not correctly describe this adsorption.

3.7.3. Temkin isotherm

Temkin isotherm takes into consideration the interaction between adsorbate and adsorbent with the consequence that the heat of adsorption of all the molecules in the layer decreases linearly with further coverage. It also assumes that the distribution of adsorbate is uniform [40]. The linear form is given as follows:

$$q_e = \frac{RT}{b} \ln A + \frac{RT}{b} \ln C_e \qquad (7)$$

Where T is the absolute temperature in Kelvin (K), R is the molar gas constant (8.314J mol^{-1} K^{-1}), A represent the equilibrium binding constant (L g^{-1}) corresponding to maximum binding energy and b ($Jmol^{-1}$) is related to the heat of adsorption. The intercept and slope from the plot of q_e versus log C_e enabled us to determine A and b as displayed in Table 3. Judging from the high value of the coefficient of determination R^2 = 0.9948, it can be concluded that Temkin isotherm model describe this equilibrium very well. This indicates the possibility of adsorbent-adsorbate interaction and the adsorption process is simply a function of surface coverage.

3.8. Energy of adsorption

The activation energy of adsorption can be computed from the Arrhenius equation presented as follows:

$$\ln k_2 = \frac{E_a}{2.303\ RT} + constant \qquad (8)$$

Where E_a ($kJmol^{-1}$) is the activation energy, k_2 (g mg^{-1} h^{-1}) is the second order rate constant as shown in Table 1 and R is the molar gas constant (8.314J mol^{-1} K^{-1}) and T is the temperature of the solution in Kelvin. Plotting lnk_2 against 1/T (Figure 7(a)) gave a linear relation whose slope (Ea/R) allowed us to determine activation energy of adsorption. From the Table 4, the activation energy is 39.29 kJmol^{-1}, which is low and therefore, is an indication of the favorability of the adsorption process.

Studies on adsorption thermodynamics have employed the ratio of qe/Ce as the distribution constants K in the Vant-Hoff equation to derive the adsorption thermodynamic parameters [41]. The modified equation is given as follows:

$$ln\left(\frac{q_e}{C_e}\right) = -\frac{\Delta H}{RT} + \frac{\Delta S}{R} \qquad (9)$$

$$\Delta G = \Delta H + T\Delta S \qquad (10)$$

Where, all the letters and symbols have their usual meanings. A plot of log (q_e/C_e) versus 1/T is depicted in Figure 7(b) and the thermodynamic parameters extracted from the plot are shown in Table 4. Looking at able 3, it is evident that as temperature climbs up from 298 to 333K, the free energy change ΔG becomes less negative meaning that as an exothermic process, it is not favored at higher temperatures. The ΔH of -43.87 kJmol^{-1} also corroborates this observation. The negative change in entropy ΔS of -110.11J mol^{-1} K^{-1} suggest a significant fall in randomness at solution-solid interface during adsorption.

Table 1. Adsorption kinetic parameters for Lagergren models

Concentration (ppm)	$q_{e,exp}$ (mg g^{-1})	Pseudo 1st order			Pseudo 2nd order			
		k_1 (h^{-1})	$q_{e,cal}$ (mg g^{-1})	R^2	$q_{e,cal}$ (mg g^{-1})	k_2 (g mg^{-1} h^{-1})	h^a (mg g^{-1} h^{-1})	R^2
10	6.63	16.4	0.606	0.9854	6.70	55.7	2.50×10^3	1.000
20	13.3	10.1	0.908	0.9450	13.3	56.7	1.00×10^4	1.000
40	26.5	2.70	1.60	0.9562	26.3	8.10	5.60×10^3	0.9999

60	39.2	6.93	8.39	0.9541	39.4	3.23	5.01×10^3	1.000
100	59.4	4.97	3.96	0.9640	59.5	2.82	9.98×10^3	1.000

---

[a] Initial adsorption rate, h = $k_2q_e^2$

Table 2. Intraparticle diffusion parameters

Intraparticle diffusion model			
Temperature (K)	k_{id} (mg g^{-1} h^{-1})	x_i (mg g^{-1})	R^2
298	2.12	24.7	0.9812
313	0.998	25.2	0.9807
333	0.413	25.1	0.9804

Table 3. Isotherm constants for adsorption of Pb^{2+} on CDAP

Adsorption Isotherms	Isotherm Parameters		R^2
Langmuir	Q_m	64.5 mg g^{-1}	0.9943
	b	2.07 L mg^{-1}	
Freundlich	k_f	34.2	0.9323
	n	2.23	
Temkin	A	34.8 Lg^{-1}	0.9948
	b	221 J mol^{-1}	

Table 4. Thermodynamic and kinetic parameters for Pb^{2+} adsorption on CDAP

Temp (K)	ΔG (kJ mol^{-1})	ΔH ($kJmol^{-1}$)	ΔS ($Jmol^{-1}$ K^{-1})	E_a ($kJmol^{-1}$)
298	-11.1			
313	-9.41	-43.9	-110	39.3
333	-7.20			

Table 5. Comparism of the adsorption capacity of the resin and those of various adsorbents in literature for Pb (II) as computed by the linear Langmuir equation.

Sorbent Materials	**Adsorption Capacity (mg/g)**	**Ref**
Commercial silica	3.9	[42]
Zeolites: Chabazite	6.0	[43]
Activated carbon	6.68	[44]
Porous lignin-based sphere	27.1	[45]
Diethylenetriamine-bacterial cellulose	31.4	[46]
Ethylenediamine modified cellulose	50.0	[47]
Porous lignin xanthate resin	62.6	[48]
Ferrihydrite	366	[49]
Lignocellulosic materials	66	[50]
Modified orange peel	210	[51]
Sulfured orange peel	164	[52]
Nanoribbon	74.6	[53]
Current Resin	64.5	This work

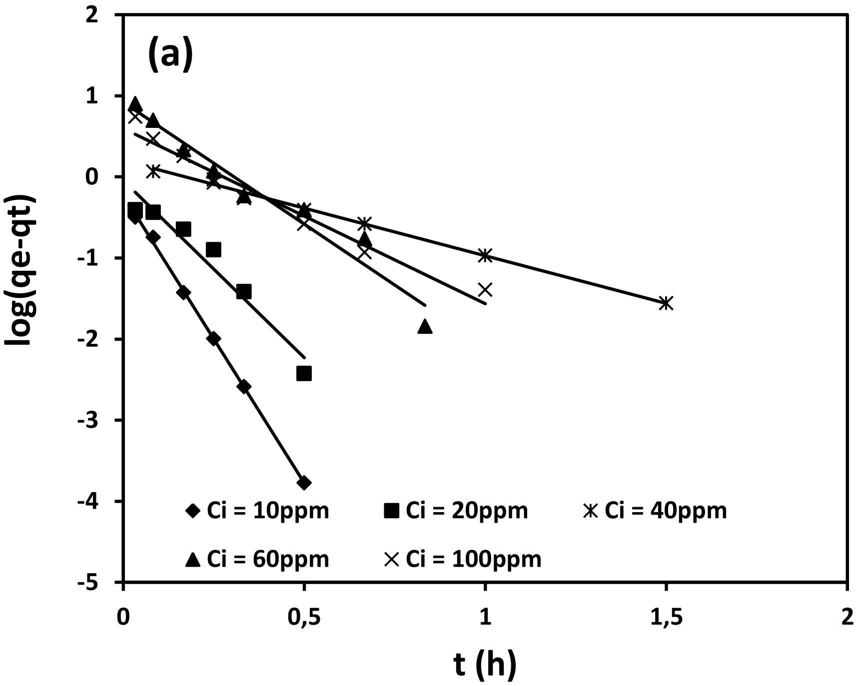
(a)
log(qe-qt)
t (h)
2
1
0
-1
-2
-3
-4
-5
0
0,5
1
1,5
2
Ci = 10ppm
Ci = 20ppm
Ci = 40ppm
Ci = 60ppm
Ci = 100ppm

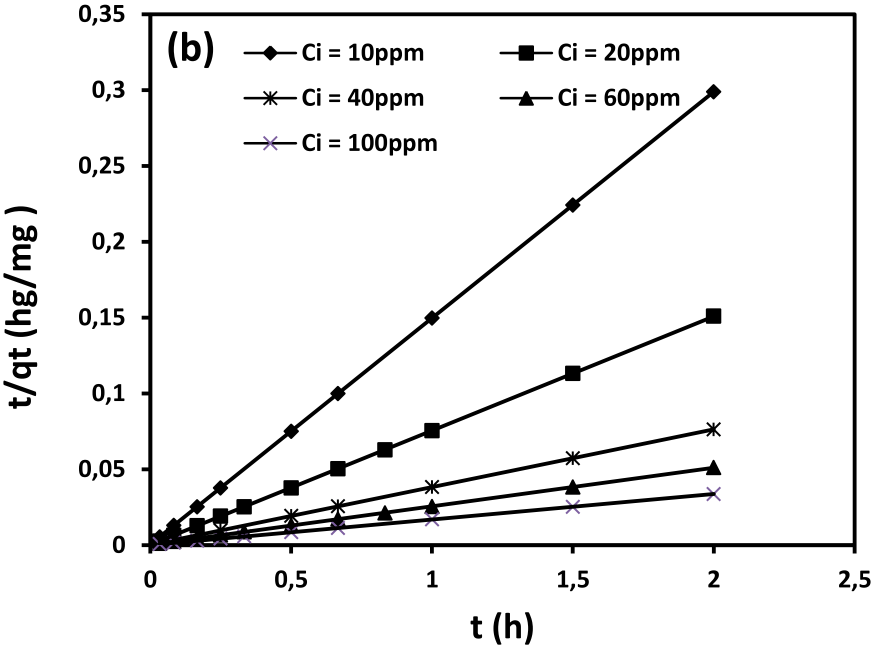

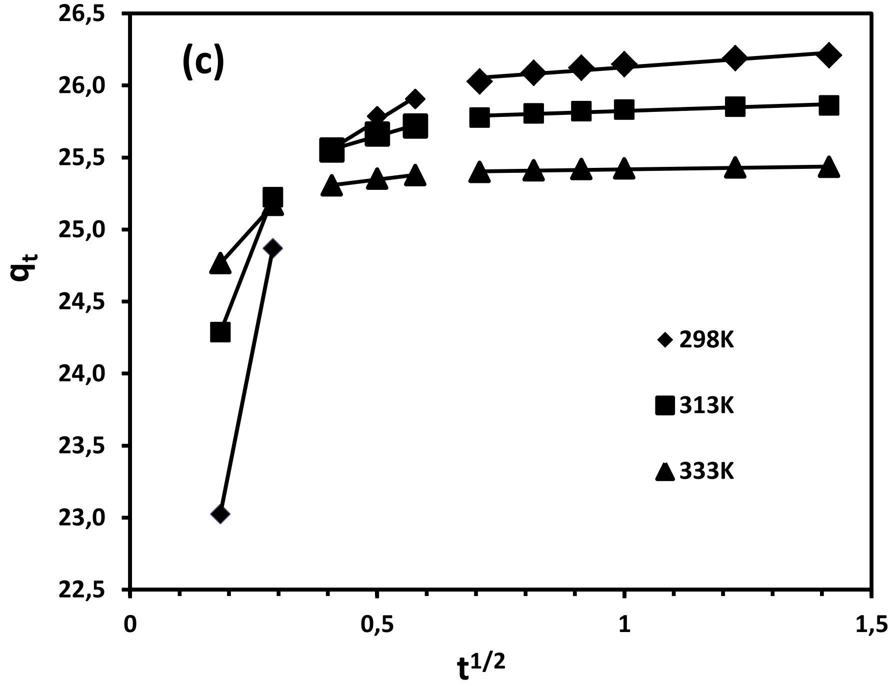

Figure 6. (a) Lagergren first-order plots, (b) Pseudo second-order plots and (c) and Weber-Morris intraparticle diffusion plots at 40 ppm for the adsorption of Pb^{2+} on CDAP

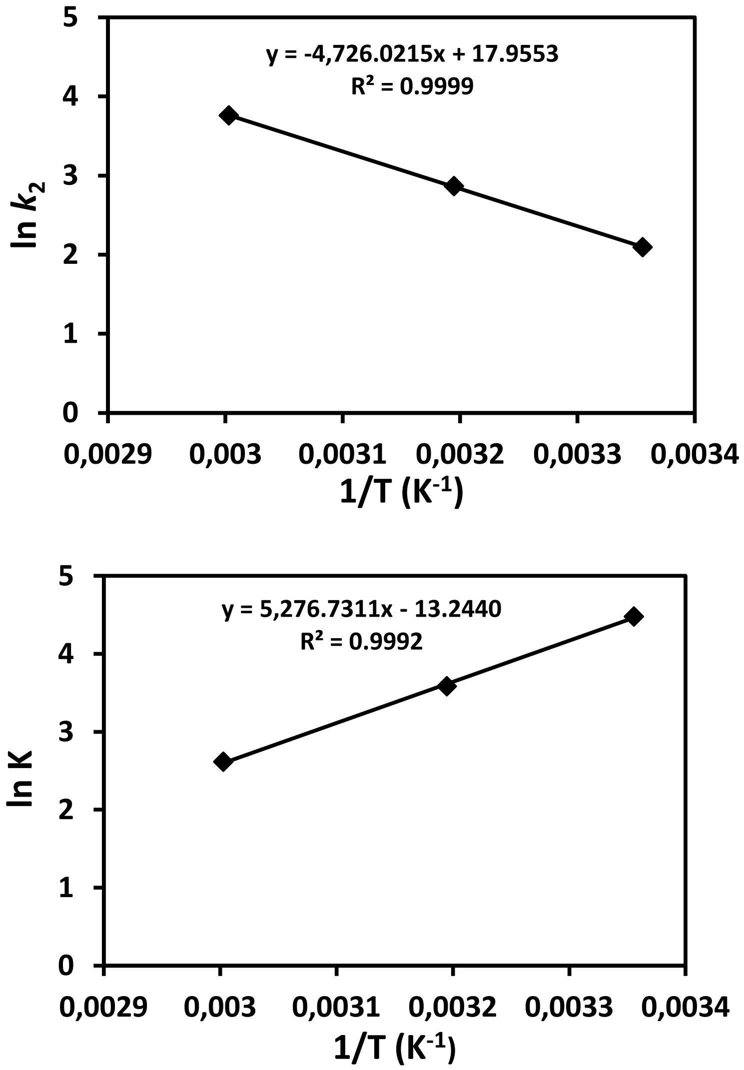

Figure 7. (a) Arrhenius and (b) Thermodynamic plots for Pb^{2+} adsorption on CDAP 4

3.8. Structure and Surface morphology of unloaded and loaded CDAP

A scanning electron microscope (SEM) and energy dispersive X-ray (EDX) analysis were performed for examining the surface morphology and the structure of the polymer before and after the adsorption, Fig.8. The EDX spectrum recorded for lead-loaded polymer adsorption (Figure 8b) indicates the main characteristic peaks for Pb(II) at 2.34 and 10.55 keV in addition to the peaks of the other elements of the polymer structure Figure (8a). This confirms the binding of Pb(II) to the surface of the polymer. SEM images are depicted in the Figures. The surface area and the pore size of the unloaded CDAP as determined by BET are 0.1627m²/g and 15.099 Å respectively. The low surface area of this efficient adsorbent may mean that chemisorption rather than just physiosorption governs the adsorption process whereby Pb^{2+} ions are captured by carboxylate and sulfone groups via chelation. As noted earlier, the increase in broadness and intensity of the IR bands of COO^- after Pb^{2+} adsorption (Fig. 1c) is a strong evidence of the attraction of the resin for Pb^{2+} ions. Evidence of interactions from IR and EDX analyses allows us to propose the following mechanism to explain the latitude of this resin for metal chelation (Scheme 2). Though Scheme 2 allows us to visualize the various plausible 5, 6, and 7-membered chemical interactions which make the resin an efficient sorbent for the removal of toxic metal ions.

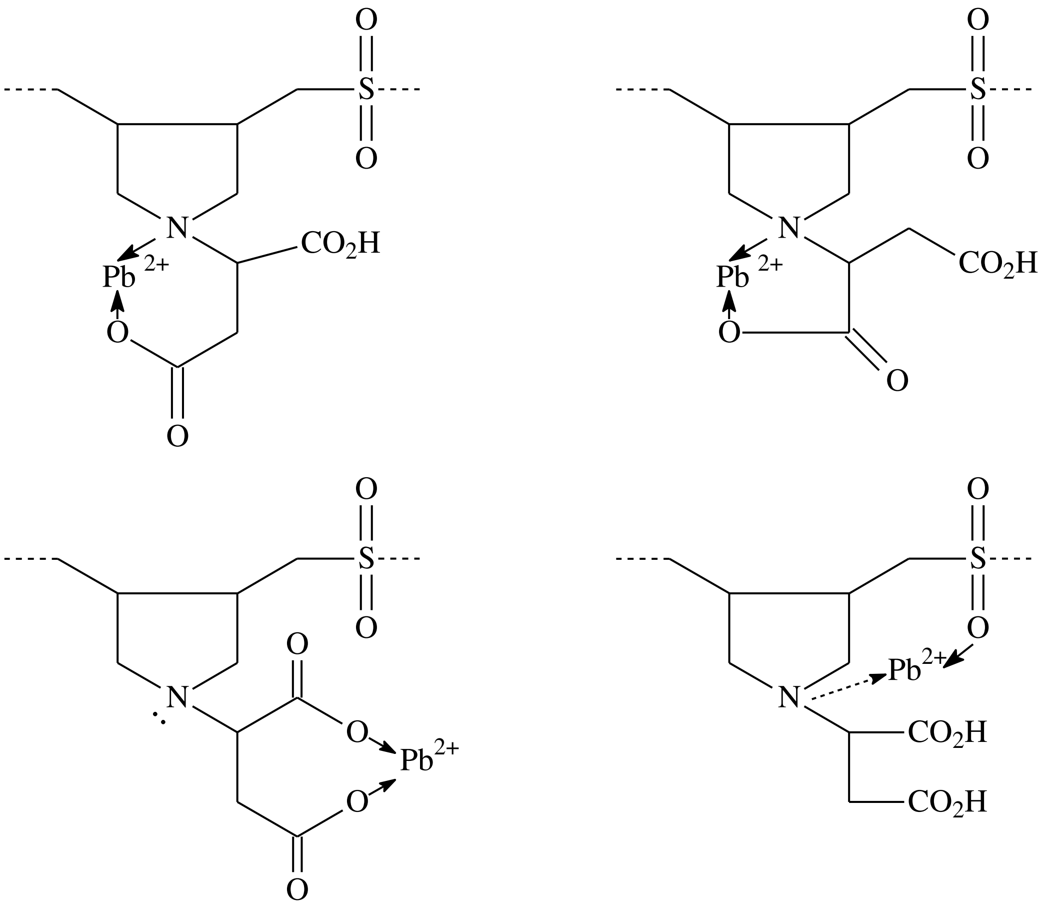

Scheme 2. Illustration of the resins's latitude in forming complex with metal ions.

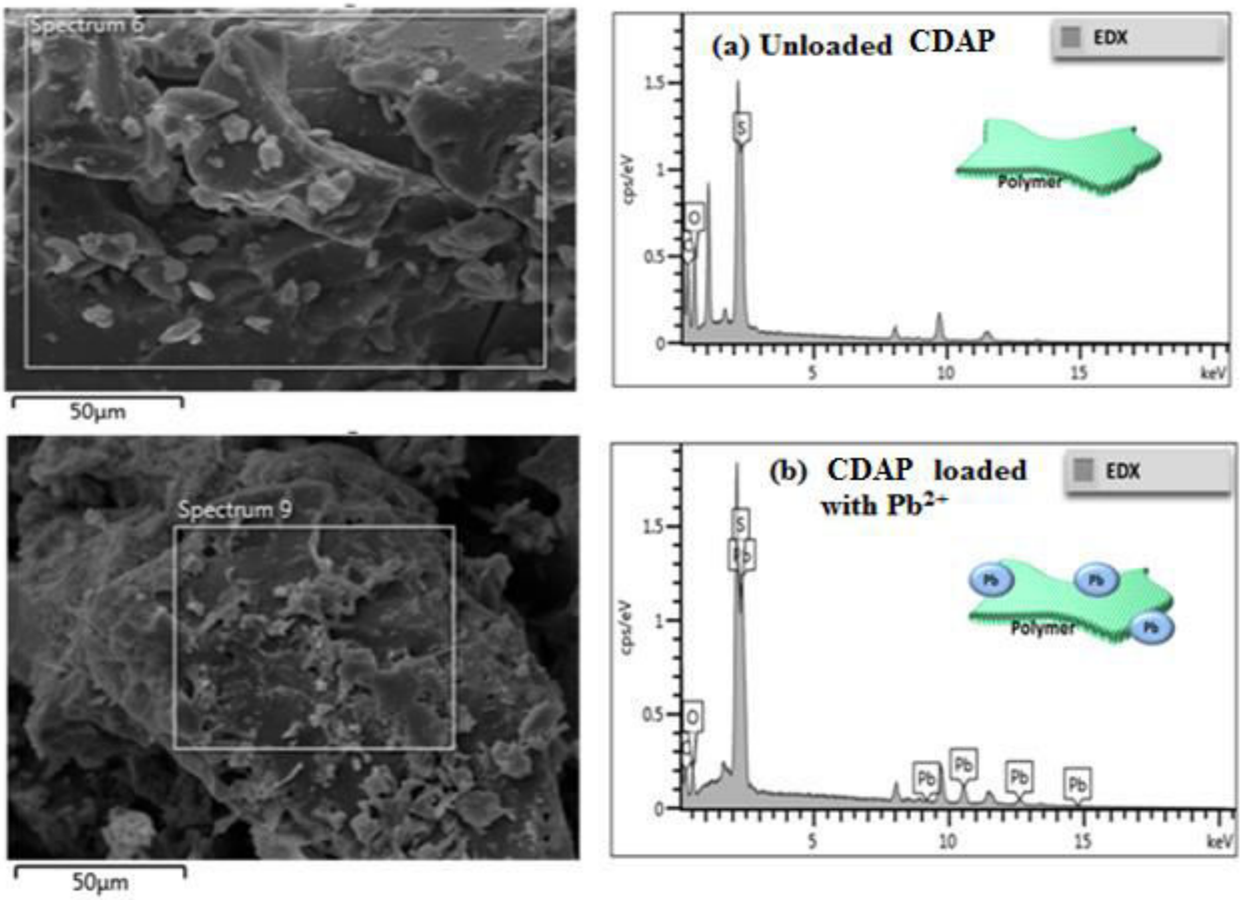

Fig. 8 . SEM image and the corresponding EDX spectrum of (a) unloaded CDAP 4 and (b) CDAP loaded with Pb^{2+} .

3.9. Regeneration and Treatment of real wastewater samples

The re-usability and safe disposal of the used resin are key factors in enhancing the environmental friendliness of the resin. The result indicated that the efficiency of regeneration stands at 96 %. The percentage lead uptake of the regenerated resin stands at 87 % as against fresh resin, which stands at 98%.

Sample of industrial wastewater collected from the industrial unit in dammam was used to study the effect of real wastewater matrix and to evaluate practical application of the polymer. The samples were spiked with 0.0 and 20 mg/L Pb(II), and then treated with polymer under the optimum conditions. Table 6 presents the ICP results of the analysis of wastewater sample and wastewater sample after being treated with the prepared polymer. It also presents the analysis of wastewater sample after being spiked with 20 ppm Pb(II) and then treated with the prepared polymer. The results indicated that the efficiency of the polymer for the adsorption of Pb(II) is hardly be influenced by the real wastewater matrix. This indicates the high efficiency and capability of polymer to be regarded as a potential adsorbent for high efficient and renewable adsorbent for Pb(II) ions from aqueous solutions.

Table 6

Comparison of Pb(II) concentrations in wastewater sample before and after the treatment with the polymer resin

Metal	**Original sample ($\mu g\ L^{-1}$)**	**Original sample spiked with 20000 ($\mu g\ L^{-1}$) Pb(II) and then treated with the adsorbent (polymer)**
Pb	0.453	357.2
Co	0.362	0.213
Cu	857.14	418.20
As	8.14	3.351
Mo	36.12	10.4
Cd	1.17	0.087
Hg	213.11	133.4

MDL: the method detection limit

Conclusion

In this work, a novel polymer was synthesized by the cyclopolymerization protocol involving monomers having unquenched nitrogen valency to get a novel functionalized resin. FTIR, EDX, TGA and SEM characterization techniques were used to confirm the structural and morphological properties of the polymer. The polymer displays an outstanding capability to remove Pb(II) ions. The optimum pH value for Pb(II) removal was 6. The linearity of the plots t/qt vs. t implies the adsorption followed the pseudo-second order rate kinetics with high adsorption capacity. The Langmuir and Temkin models give a better correlation coefficient with

R^2 of 0.99. Langmuir monolayer adsorption capacity was 64.5 mg/g. Thermodynamic parameters were evaluated; the negative values of ΔG^o indicate the spontaneity and the negative values of ΔH^o (-43.87 KJ/mol) showed the exothermic nature of Pb(II) sorption on the polymer. Therefore, the polymer adsorbent could be considered as a potential adsorbent of high efficient for Pb (II) removal.

ACKNOWLEDGEMENTS

The authors gratefully acknowledge the support provided by King Abdulaziz City for Science and Technology (KACST) through the Science & Technology Unit at King Fahd University of Petroleum & Minerals (KFUPM) for funding this work through project No. 11-ADV2132-04 as part of the National Science, Technology and Innovation Plan and the facilities provided by KFUPM.

References

1. Heidari, A., H. Younesi, and Z. Mehraban, Removal of Ni(II), Cd(II), and Pb(II) from a ternary aqueous solution by amino functionalized mesoporous and nano mesoporous silica. Chemical Engineering Journal, 2009. 153(1–3): p. 70-79.
2. (EPA), E.P.A., Environmental Pollution Control Alternatives. 1990(EPA/625/5-90/025, EPA/625/4-89/023).
3. Jiang, M.-q., et al., Removal of Pb(II) from aqueous solution using modified and unmodified kaolinite clay. Journal of Hazardous Materials, 2009. 170(1): p. 332-339.
4. Rao, M.M., et al., Removal of some metal ions by activated carbon prepared from Phaseolus aureus hulls. Journal of Hazardous Materials, 2009. 166(2–3): p. 1006-1013.
5. Ghaedi, M., et al., Comparison of the efficiency of palladium and silver nanoparticles loaded on activated carbon and zinc oxide nanorods loaded on activated carbon as new adsorbents for removal of Congo red from aqueous solution: Kinetic and isotherm study. Materials Science and Engineering: C, 2012. 32(4): p. 725-734.
6. Dias, J.M., et al., Waste materials for activated carbon preparation and its use in aqueous-phase treatment: A review. Journal of Environmental Management, 2007. 85(4): p. 833-846.
7. Erdem, E., N. Karapinar, and R. Donat, The removal of heavy metal cations by natural zeolites. Journal of Colloid and Interface Science, 2004. 280(2): p. 309-314.

8. Liu, J., et al., Novel negatively charged hybrids. 3. Removal of Pb2+ from aqueous solution using zwitterionic hybrid polymers as adsorbent. Journal of Hazardous Materials, 2010. 173(1–3): p. 438-444.

9. Liu, J., et al., Preparation of zwitterionic hybrid polymer and its application for the removal of heavy metal ions from water. Journal of Hazardous Materials, 2010. 178(1–3): p. 1021-1029.

10. Liu, J., et al., Novel negatively charged hybrids. 1. copolymers: Preparation and adsorption properties. Separation and Purification Technology, 2009. 66(1): p. 135-142.

11. Cegłowski, M. and G. Schroeder, Preparation of porous resin with Schiff base chelating groups for removal of heavy metal ions from aqueous solutions. Chemical Engineering Journal, 2015. 263(0): p. 402-411.

12. Butler, G.B., Cyclopolymerization and cyclocopolymerization. Marcel Dekker, New York 1992.

13. P. K. Singh, V.K.S., M. Singh, E-Polymers, 2007. 030: p. 1-34.

14. S. Kudaibergenov, W.J., A. Laschewsky, Adv. Polym. Sci., 2006. 201: p. 157-224

15. Jaeger, W., J. Bohrisch, and A. Laschewsky, Synthetic polymers with quaternary nitrogen atoms—Synthesis and structure of the most used type of cationic polyelectrolytes. Progress in Polymer Science, 2010. 35(5): p. 511-577.

16. Ali, S.A. and O.C.S. Al-Hamouz, Comparative solution properties of cyclocopolymers having cationic, anionic, zwitterionic and zwitterionic/anionic backbones of similar degree of polymerization. Polymer, 2012. 53(15): p. 3368-3377.

17. Abu-Thabit, N.Y., et al., Phosphonobetaine/sulfur dioxide copolymer by Butler's cyclopolymerization process. European Polymer Journal, 2011. 47(5): p. 1113-1123.

18. Ali, S.A., et al., Synthesis and comparative solution properties of single-, twin-, and triple-tailed associating ionic polymers based on diallylammonium salts. Journal of Polymer Science Part A: Polymer Chemistry, 2006. 44(19): p. 5480-5494.

19. Butler, G.B., Cyclopolymerization. Journal of Polymer Science Part A: Polymer Chemistry, 2000. 38(19): p. 3451-3461.

20. McGrew, F.C., J. Chem., 1958. 35: p. 178-186.

21. Ali, S.A., S.Z. Ahmed, and E.Z. Hamad, Cyclopolymerization studies of diallyl-and tetraallylpiperazinium salts. Journal of Applied Polymer Science, 1996. 61(7): p. 1077-1085.

22. Al-Muallem, H.A., M.I.M. Wazeer, and S.A. Ali, Synthesis and solution properties of a new pH-responsive polymer containing amino acid residues. Polymer, 2002. 43(15): p. 4285-4295.

23. Silvia Martínez-Tapia, H., et al., Synthesis and Structure of Na2[(HO3PCH2)3NH]1.5H2O: The First Alkaline Triphosphonate. Journal of Solid State Chemistry, 2000. 151(1): p. 122-129.

24. D. Kołodynska, Z.H.a.S.P.-P., FT-IR/PAS Studies of Cu(II)–EDTA Complexes Sorption on the Chelating Ion Exchangers. ACTA PHYSICA POLONICA A, 2009. 116(3): p. 340-343.

25. Plazinski, W. and W. Rudzinski, Modeling the Effect of pH on Kinetics of Heavy Metal Ion Biosorption. A Theoretical Approach Based on the Statistical Rate Theory. Langmuir, 2008. 25(1): p. 298-304.

26. W.D. Schecher, D.C.M., MINEQL+: a chemical equilibrium program for personal computers (Version 4.5). Environmental Research Software, Hallowell, Maine, USA, 2001.

27. Liu, W.-J., et al., Adsorption of lead (Pb) from aqueous solution with Typha angustifolia biomass modified by SOCl2 activated EDTA. Chemical Engineering Journal, 2011. 170(1): p. 21-28.

28. Aroua, M.K., et al., Real-time determination of kinetics of adsorption of lead(II) onto palm shell-based activated carbon using ion selective electrode. Bioresource Technology, 2008. 99(13): p. 5786-5792.

29. S. Lagergren, K.S., Vetenskapsakad, Handl., 1898. 24: p. 1–39.

30. Ho, Y.S. and G. McKay, Comparative sorption kinetic studies of dye and aromatic compounds onto fly ash. Journal of Environmental Science and Health, Part A, 1999. 34(5): p. 1179-1204.

31. Ho, Y.S. and G. McKay, Pseudo-second order model for sorption processes. Process Biochemistry, 1999. 34(5): p. 451-465.

32. Minceva, M., L. Markovska, and V. Meshko, Removal of Zn 2+ , Cd 2+ and Pb 2+ from binary aqueous solution by natural zeolite and granulated activated carbon. 2007. Vol. 26. 2007.

33. W.J. Weber, J.C.M., Eng. Div. Am. Soc. Civ. Eng., 1963. 89: p. 31–60.

34. Annadurai, G., R.-S. Juang, and D.-J. Lee, Use of cellulose-based wastes for adsorption of dyes from aqueous solutions. Journal of Hazardous Materials, 2002. 92(3): p. 263-274.

35. Vergili, I., et al., Study of the Removal of Pb(II) Using a Weak Acidic Cation Resin: Kinetics, Thermodynamics, Equilibrium, and Breakthrough Curves. Industrial & Engineering Chemistry Research, 2013. 52(26): p. 9227-9238.

36. Wu, F.C., R.L. Tseng, and R.S. Juang, Adsorption of Dyes and Phenols from Water on the Activated Carbons Prepared from Corncob Wastes. Environmental Technology, 2001. 22(2): p. 205-213.

37. Rengaraj, S., et al., Adsorption characteristics of Cu(II) onto ion exchange resins 252H and 1500H: Kinetics, isotherms and error analysis. Journal of Hazardous Materials, 2007. 143(1–2): p. 469-477.

38. Langmuir, I., THE ADSORPTION OF GASES ON PLANE SURFACES OF GLASS, MICA AND PLATINUM. Journal of the American Chemical Society, 1918. 40(9): p. 1361-1403.

39. Freundlic, H.M.F., Uber die adsorption in losungen. Zeitschrift fur Physikalische Chemie (Leipzig), 1906. 57A: p. 385–470.

40. M.J. Tempkin, V.P.J.T., V. Pyzhev,, Acta Physiochim URSS, 1940: p. 217–222.

41. Sheha, R.R. and A.A. El-Zahhar, Synthesis of some ferromagnetic composite resins and their metal removal characteristics in aqueous solutions. Journal of Hazardous Materials, 2008. 150(3): p. 795-803.

42. Chiron, N., R. Guilet, and E. Deydier, Adsorption of Cu(II) and Pb(II) onto a grafted silica: isotherms and kinetic models. Water Research, 2003. 37(13): p. 3079-3086.

43. Ouki, S.K. and M. Kavannagh, PERFORMANCE OF NATURAL ZEOLITES FOR THE TREATMENT OF MIXED METAL-CONTAMINATED EFFLUENTS. Waste Management & Research, 1997. 15(4): p. 383-394.

44. Mishra, P.C. and R.K. Patel, Removal of lead and zinc ions from water by low cost adsorbents. Journal of Hazardous Materials, 2009. 168(1): p. 319-325.

45. Li, Z., Y. Ge, and L. Wan, Fabrication of a green porous lignin-based sphere for the removal of lead ions from aqueous media. Journal of Hazardous Materials, 2015. 285(0): p. 77-83.

46. Shen, W., et al., Adsorption of Cu(II) and Pb(II) onto diethylenetriamine-bacterial cellulose. Carbohydrate Polymers, 2009. 75(1): p. 110-114.

47. Musyoka, S.M., et al., Synthesis, Characterization, and Adsorption Kinetic Studies of Ethylenediamine Modified Cellulose for Removal of Cd and Pb. Analytical Letters, 2011. 44(11): p. 1925-1936.

48. Li, Z., Y. Kong, and Y. Ge, Synthesis of porous lignin xanthate resin for Pb2+ removal from aqueous solution. Chemical Engineering Journal, 2015. 270(0): p. 229-234.

49. K. Rout, M. Mohapatra and S. Anand, 2-Line ferrihydrite: synthesis, characterization and its adsorption behaviour for removal of Pb(II), Cd(II), Cu(II) and Zn(II) from aqueous solutions, Dalton Trans., 2012, 41, 3302-3312

50. I. Anastopoulos, I. Massas, C. Ehaliotis, Composting improves biosorption of Pb2+ and Ni2+ by renewable lignocellulosic materials. Characteristics and mechanisms involved, Chemical Engineering Journal, 231, 2013, 245–254

51. FENG Ning-chuan, GUO Xue-yi, Characterization of adsorptive capacity and mechanisms on adsorption of copper, lead and zinc by modified orange peel Trans. Nonferrous Met. Soc. China 22(2012) 1224−1231

52. Sha Liang, Xueyi Guo, , Qinghua Tian, Adsorption of Pb2+ and Zn2+ from aqueous solutions by sulfured orange peel, Desalination, 275, 2011, 212–216

53. Li Yu, Rujia Zou, Zhenyu Zhang , Guosheng Song , Zhigang Chen , Jianmao Yang and Junqing Hu, A Zn2GeO4–ethylenediamine hybrid nanoribbon membrane as a recyclable adsorbent for the highly efficient removal of heavy metals from contaminated water, Chem. Commun., 2011, 47, 10719-10721

54. Phoebe Zito Ray and Heather J. Shipley, Inorganic nano-adsorbents for the removal of heavy metals and arsenic: a review, RSC Adv., 2015,5, 29885-29907

55. Susmita Sen Gupta and Krishna G. Bhattacharyya, Adsorption of metal ions by clays and inorganic solids, RSC Adv., 2014,4, 28537-28586

56. Yongshun Huang, Jiaxing Li, Xiaoping Chen and Xiangke Wang, Applications of conjugated polymer based composites in wastewater purification, RSC Adv., 2014,4, 62160-62178

Table of contents

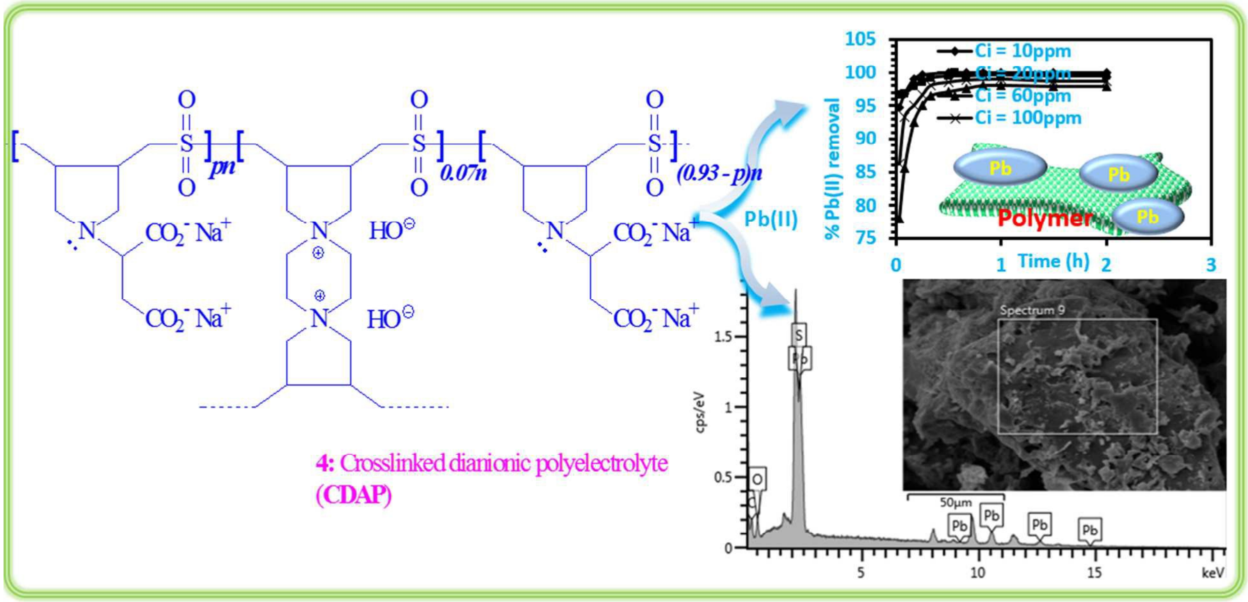

Aspartic acid-based novel adsorbent containing basic nitrogen as well as two carboxyl motifs as effective metal-chelation centers